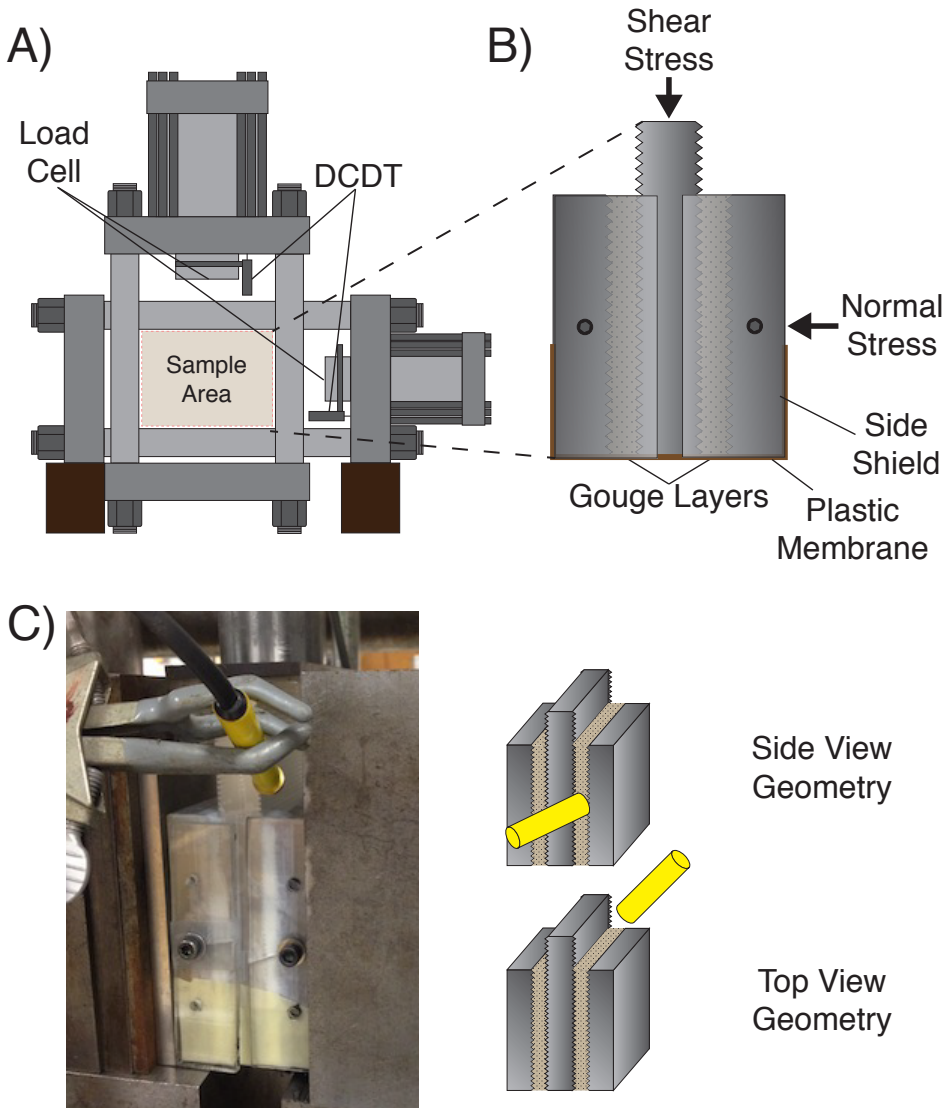

Figure 1. Experimental setup. A) The biaxial hydraulic press: sample assemblies are supported by steel blocks in the sample area. B) Double direct shear geometry consists of two layers of gouge confined between three forcing blocks. Side shields and a plastic membrane are used to contain gouge material as the sample is sheared. C) Placement of the electrostatic voltmeter (yellow cylinder) in the side and top view positions. A window was cut into the side shield for the side view geometry.

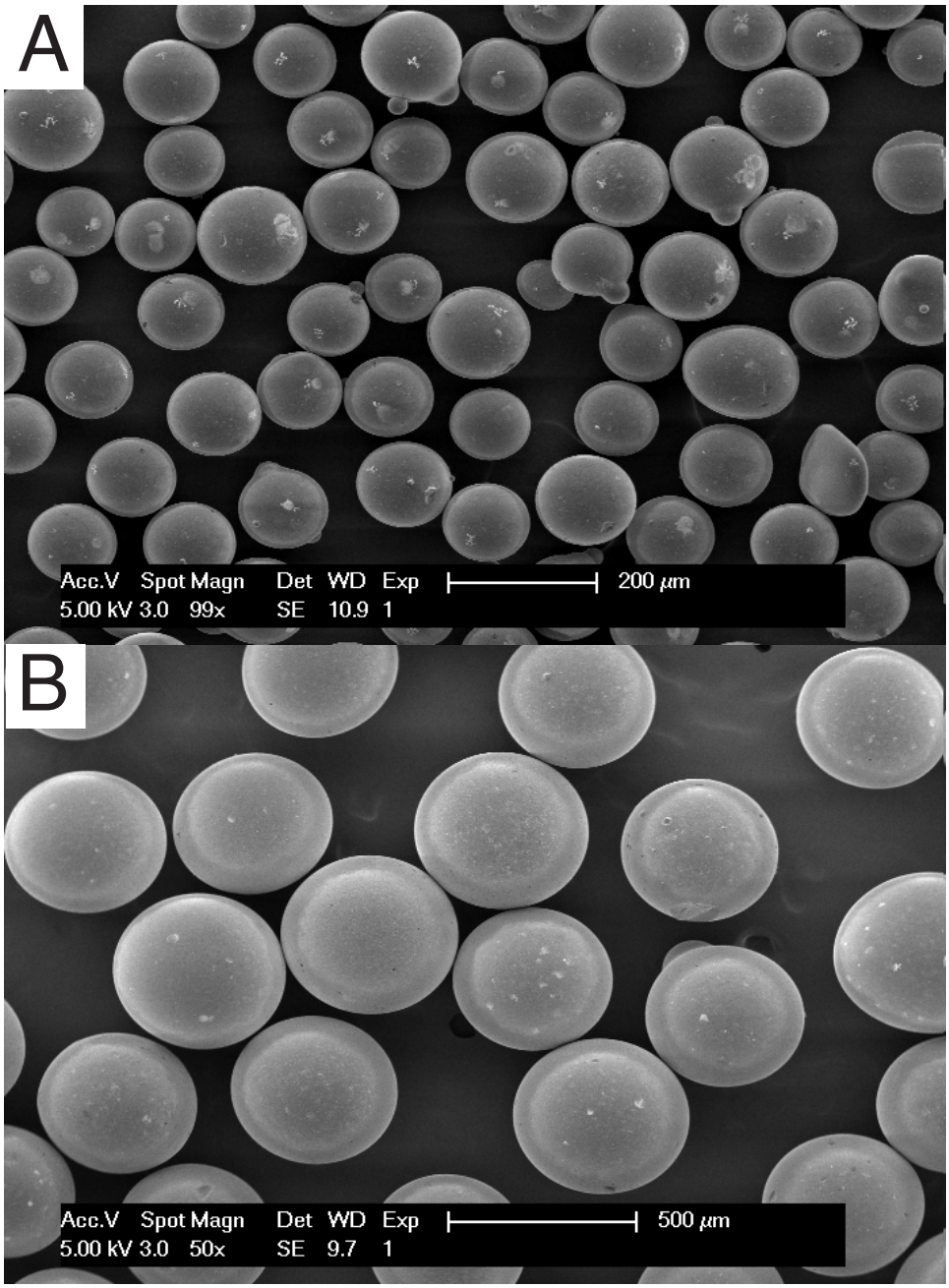

Figure 2. Scanning electron microscope micrographs of the starting glass beads for all experiments. A) 100-150 μm B) 420-500 μm

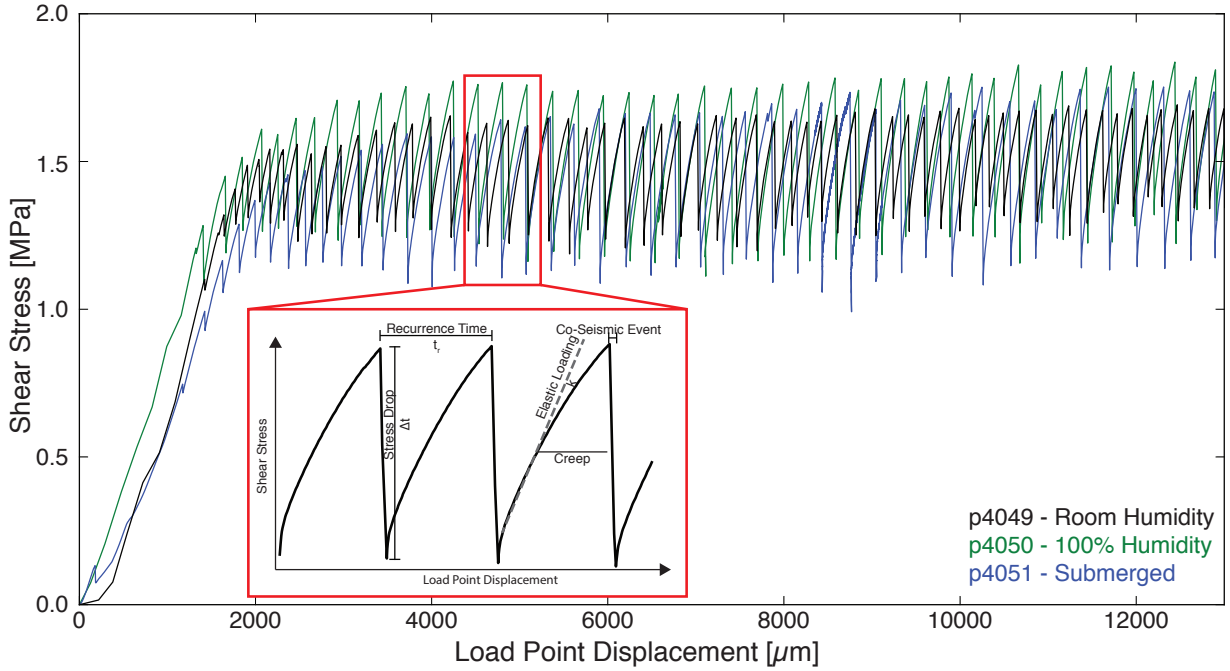

Figure 3. Experiments performed on glass beads (100-150μm diameter) under ambient humidity, 100% humidity, and submerged conditions exhibit similar mechanical behavior. Increased stress drops are observed with increased humidity and in the submerged case. Inset: Anatomy of a stick-slip event. The recurrence time is the time between peaks in shear stress. Initially the shear stress increases linear-elastically. Deviation from line-elastic behavior marks the onset of elasto-plastic deformation and pre-seismic slip. When the ultimate strength of the layer is reached shear stress drops rapidly and the cycle begins again.

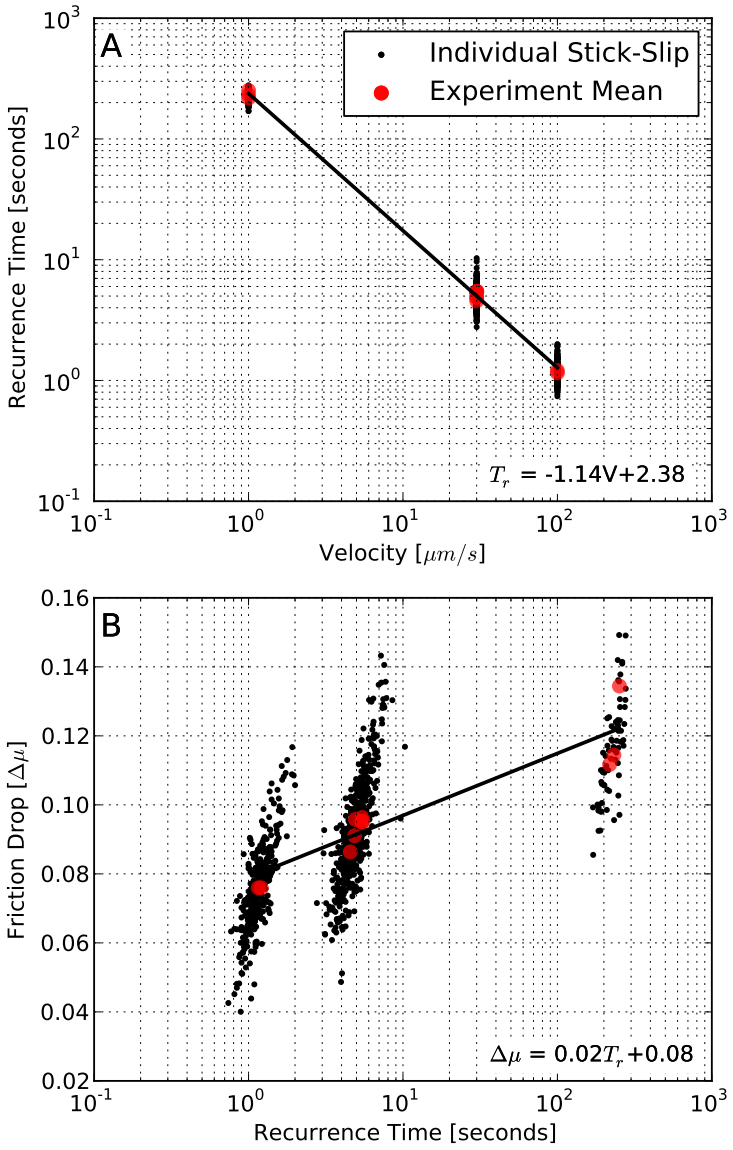

Figure 4. A) Samples exhibit a log-log linear relation between recurrence time and velocity. Faster loading rates result in shorter recurrence times. B) Friction drop increases with the recurrence time as there is more time for the layer to heal before the next stick-slip event.

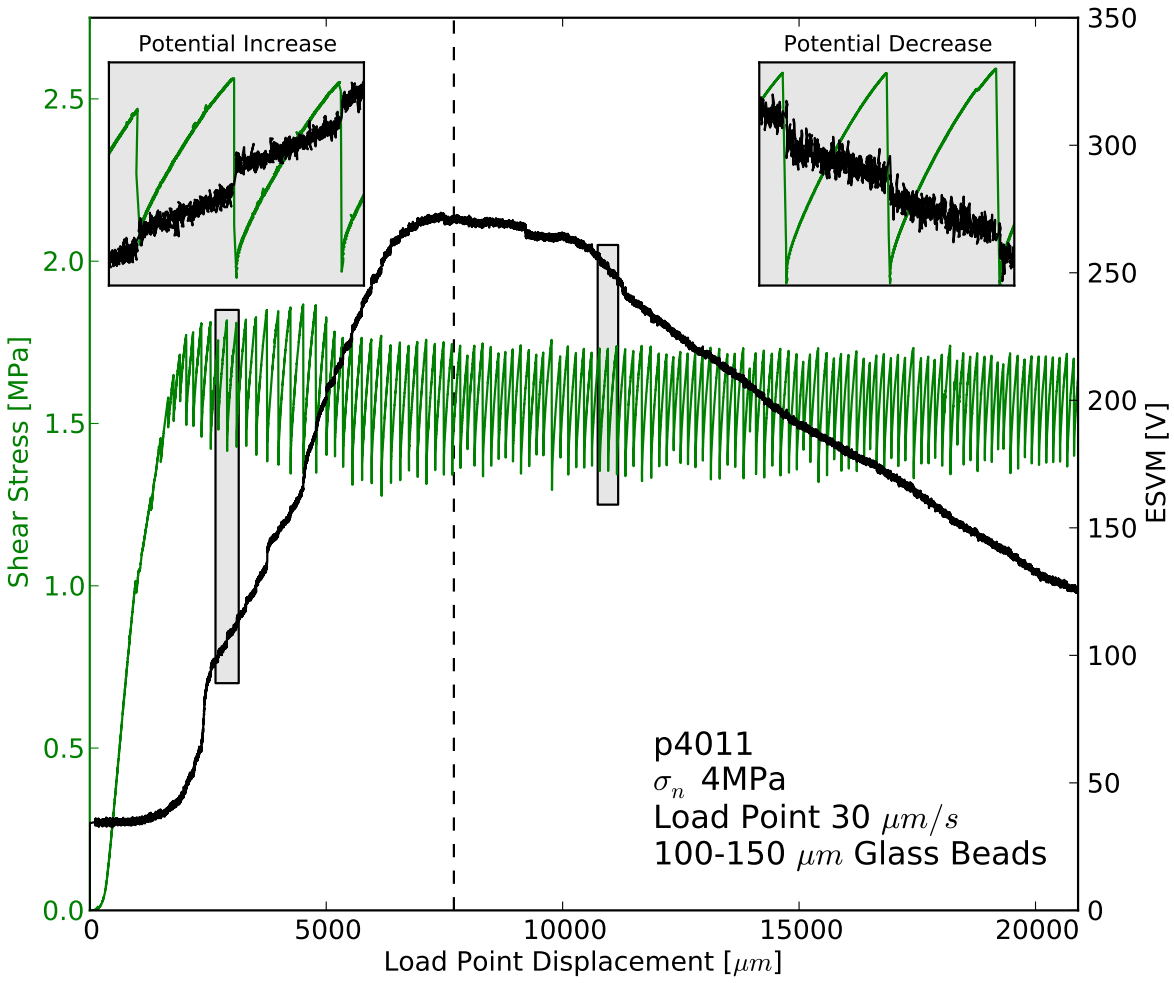

Figure 5. During shearing two trends are observed: 1) A long-term charging/discharging trend in the electrical potential and 2) Potential change related to individual stick-slip events. The entire system initially charges, approximately until mechanical steady-state is reached. During this phase co-seismic potential changes are dominantly positive (top left inset). After attainment of mechanical steady-state, the system begins to maintain or discharge potential. During this phase the co-seismic potential changes are dominantly negative (top right inset).

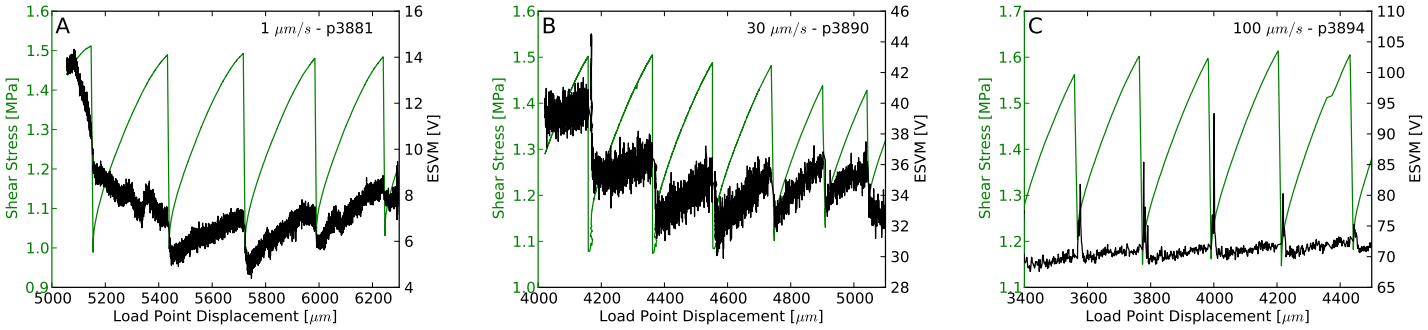

Figure 6. Stick-slip events and associated ESVM measurements for three-different load point velocities of 1,30, and 100 $\mu m/s$. A) At slow loading velocities the electrical signal clearly mirrors the stress curve in most cases B) For intermediate velocities, the relation is still present. C) At high velocities, the electrical signal is a sharp pulse an order of magnitude higher than those observed at low velocities, and we observe small inter-seismic charging.

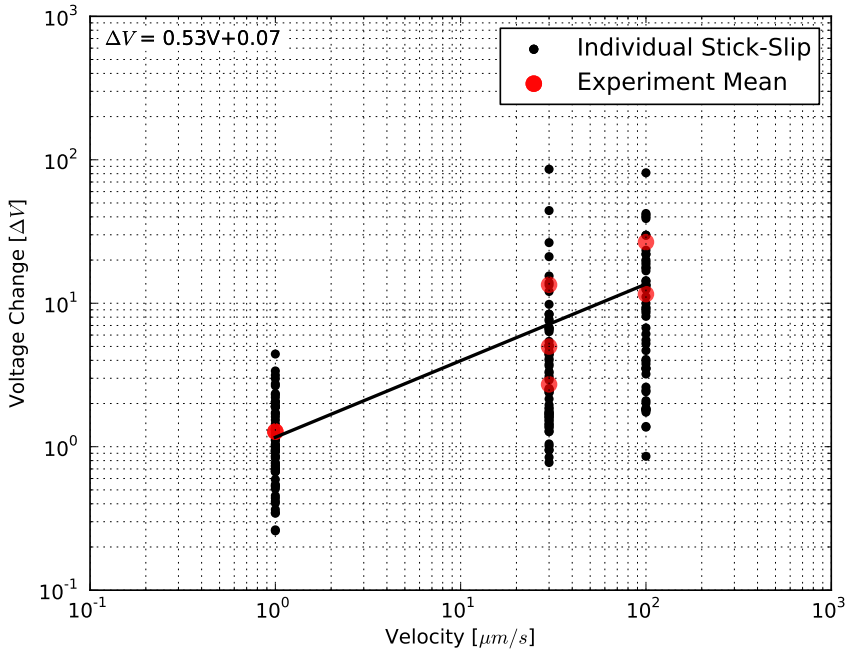

Figure 7. Each order of magnitude driving velocity change produces a ∼5x increase in the electrical signal observed. All experiments shown are with the side-view sensor geometry.

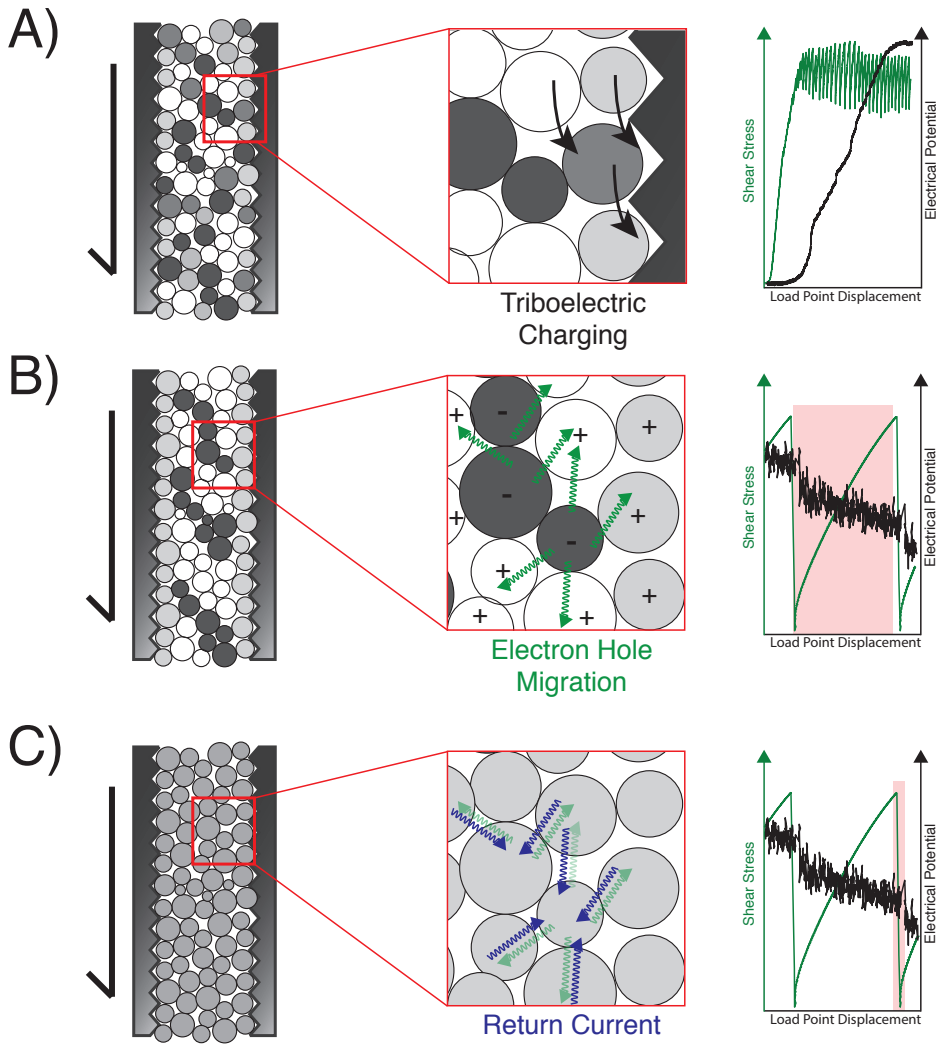

Figure 8. A schematic representation of the stages of electrical behavior during an experiment: A) During the initial run-in there is massive grain rearrangement as force chain networks begin to form. This sliding motion tribo-electrically charges the system. B) After the force chain network forms there is minimal grain-boundary sliding. Shear loads are supported in the granular layer by highly stressed force chains (dark colors). Electron holes migrate away from highly stressed beads into the matrix creating an electrical potential gradient. C) When the layer fails and all grains are at roughly the same low stress, a return current redistributes the electrical gradient and the cycle begins again.

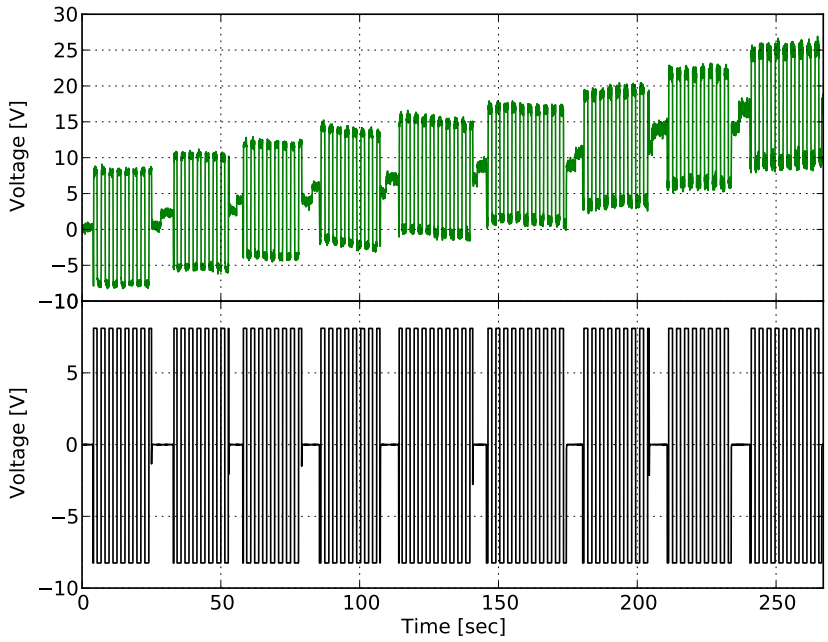

Figure 9. Calibration of the ESVM from a function generator source (bottom panel). A series of steps through the ESVM 'response' setting from 1-9 shows that the input square wave applied to the aluminium surface under test is well-recorded on each setting (top panel). The upward trend in ESVM data is a product of a DC offset that occurs each time the response setting is changed on the instrument.

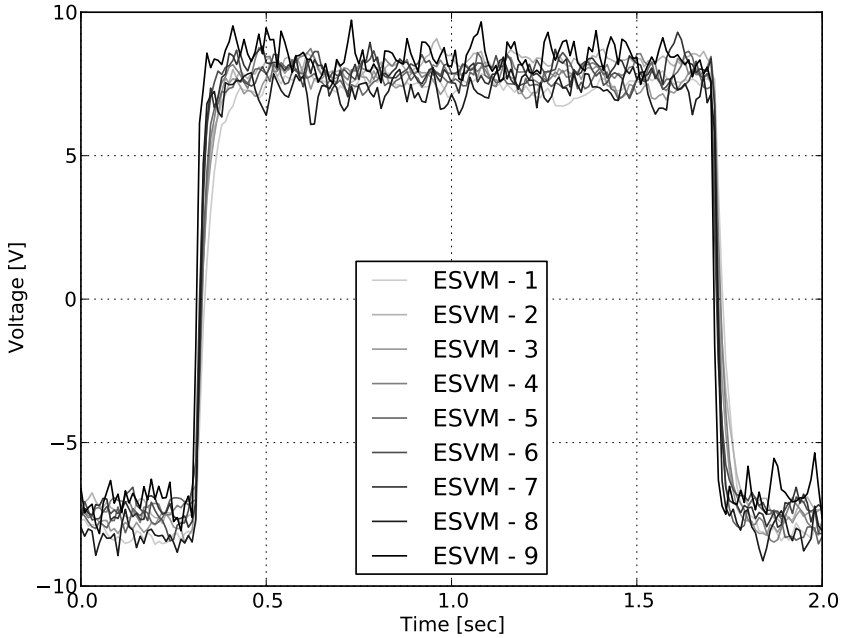

Figure 10. A detailed comparison of a single waveform shows that at lower response settings (lighter colors) the waveform is smoothed slightly, with the nearly instantaneous voltage change distributed over up to 0.1 seconds on both the rise and fall. At higher resolutions (darker colors) the sharp transition is clearly seen, but at the price of a higher noise level during the flat hold states.

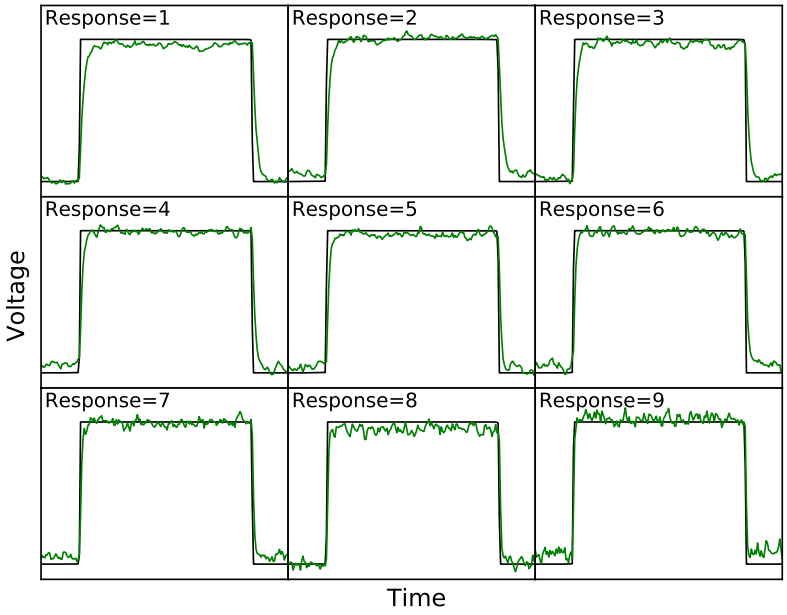

Figure 11. At all response settings the beginning of ESVM signal change corresponds well in the time domain with the leading and falling edge of the input signal. Smoothing due to longer integration times is observed at low response settings.